

This article was downloaded by: [Tomsk State University of Control Systems and Radio]

On: 23 February 2013, At: 05:57

Publisher: Taylor & Francis

Informa Ltd Registered in England and Wales Registered Number: 1072954

Registered office: Mortimer House, 37-41 Mortimer Street, London W1T 3JH, UK



## Molecular Crystals and Liquid Crystals

Publication details, including instructions for authors and subscription information:

<http://www.tandfonline.com/loi/gmcl16>

## Molecular Order Induced by Cell Walls: Part I, Experimental Results

G. J. Sprokel<sup>a</sup>

<sup>a</sup> IBM Research Laboratory, San Jose, California, 95193

Version of record first published: 28 Mar 2007.

To cite this article: G. J. Sprokel (1977): Molecular Order Induced by Cell Walls: Part I, Experimental Results, *Molecular Crystals and Liquid Crystals*, 42:1, 233-248

To link to this article: <http://dx.doi.org/10.1080/15421407708084510>

PLEASE SCROLL DOWN FOR ARTICLE

Full terms and conditions of use: <http://www.tandfonline.com/page/terms-and-conditions>

This article may be used for research, teaching, and private study purposes. Any substantial or systematic reproduction, redistribution, reselling, loan, sub-licensing, systematic supply, or distribution in any form to anyone is expressly forbidden.

The publisher does not give any warranty express or implied or make any representation that the contents will be complete or accurate or up to date. The accuracy of any instructions, formulae, and drug doses should be independently verified with primary sources. The publisher shall not be liable for any loss, actions, claims, proceedings, demand, or costs or damages

whatsoever or howsoever caused arising directly or indirectly in connection with or arising out of the use of this material.

# Molecular Order Induced by Cell Walls

## Part I, Experimental Results†

G. J. SPROKEL

*IBM Research Laboratory, San Jose, California 95193*

*(Received January 21, 1977; in final form April 21, 1977)*

Coatings or surface changes produced by exposure to r.f. plasma's have a profound effect on liquid crystal alignment. Oxide type surfaces ( $\text{SiO}_2$ ,  $\text{SnO}_2$ ,  $\text{In}_2\text{O}_3$ ) produce parallel alignment. Fluoride type surfaces (F. etched glass, fluorocarbon polymers) produce perpendicular alignment.  $\epsilon(\text{H})$  data are analyzed using conventional theory. The theory fails for mixed aligned cells but shows good agreement for all-parallel and all-perpendicular alignment.

## INTRODUCTION

Glass surfaces are altered chemically by exposure to free radicals produced in an upstream r.f. plasma and such surfaces have unexpected effects on the alignment of liquid crystals. For example, a 12-micron thick cell made from glass substrates exposed to O· free radicals produced in an  $\text{O}_2$  plasma will be parallel aligned while the same glass exposed to F· and  $\text{CF}_3\cdot$  from a  $\text{CF}_4$  plasma will cause perpendicular alignment. Noble metal surfaces which do not show preferred alignment can be changed by depositing very thin films of polymers or metal oxides using r.f. plasma techniques. Either type of alignment can be obtained. This paper deals with the alignment characteristics of surfaces prepared by free radical etching or deposition techniques. The emphasis is on the liquid crystal layer, the methods used to produce plasmas which either etch or deposit have been discussed in an accompanying paper.<sup>1</sup> For r.f. plasma techniques in general, the reader is referred to existing monographs.<sup>2</sup> Recently I. Haller reviewed<sup>3</sup> the existing literature on surface alignment. There is little to add to this review except for mentioning that previous

† Presented at the Sixth International Liquid Crystal Conference, August 1976 at Kent State University, Kent, Ohio.

efforts have, by and large, relied on surfactants. Since most surfactants are sufficiently soluble in liquid crystal materials, one cannot be sure that the alignment is caused only by surface forces. In this paper solid films are used, insoluble in the liquid crystal material.

## EXPERIMENTAL TECHNIQUES

Commercial equipment<sup>4</sup> was modified for this application. An important feature is that the sample surface is never exposed to the plasma itself thus avoiding surface changes by electron or ion bombardment. Thus, the apparatus is basically different from that described by J. C. Dubois, *et al.*<sup>5</sup> Surface changes are entirely chemical, polymers are produced *in situ* rather than in the plasma.

The type of alignment, parallel with the surface ("homogeneous") or perpendicular to it ("homeotropic") is, of course, immediately obvious by examination in polarized light. The degree of alignment is obtained by measuring the permittivity of the liquid crystal layer as a function of temperature while the sample is held in a magnetic field either opposing or enhancing the surface induced orientation. Cell capacitance and resistance are determined from amplitude and phase measurements. Test cells are made from glass substrates by standard evaporation and photolithographic techniques as described before.<sup>6</sup> The circular electrode is of 1 cm diameter and connected to a 0.125 cm wide terminal lead. One side of the cell is connected to an audio generation (G.R. 1310) through a low impedance network. The other side is connected to a source follower minimizing stray capacitance. The cell and the input impedance of the source follower form a series circuit. Phase and amplitude of the source follower output are compared with those of the generator using a H.P. type 3575 Gain/Phase meter. Conversion of the data to cell capacitance and resistance is made through an APL program considering the test cell as a parallel R/C combination. Compared with bridge measurements, this technique is much faster. The accuracy is about 1% determined mainly by the Gain/Phaser meter. The frequency is variable between 2 Hz and 2 MHz and this feature is used to determine whether the cell can indeed be represented by an R/C network. Deposited aligning layers are in fact blocking layers and cause some phase shift. From the frequency response one can determine the resistance and capacitance of the insulating layer. Data presented below all refer to the liquid crystal material proper.

The thermostat for these cells is a double walled aluminum box with a strip heater between the walls. The cell itself is suspended inside minimizing thermal contact with the walls. The cell is heated by air convection assuring uniform temperature. The temperature is measured using a calibrated

thermistor fastened to the cell. The control is proportional over about 1°C. The temperature is reproducible to about 0.05°C.

The liquid crystals used in this study are *n*-alkylcyanobiphenyls, from pentyl to nonyl. Only data for *n*-octylcyanobiphenyl are used to permit direct comparison of the surface effects. No difference was observed in alignment characteristics among these materials. Most compounds are commercially available from BDH; others were synthesized. The BDH material was used as received. The room temperature conductivity is 0.2 to  $1 \times 10^{-10}$  ohm cm<sup>-1</sup>. Low temperature vacuum drying usually decreased the conductivity but the effect is small and the drying step was omitted.

## RESULTS

### 1 Perpendicular alignment

A brief exposure of borosilicate or aluminosilicate glass surfaces to F· and CF<sub>3</sub> produced in an upstream CF<sub>4</sub> plasma will yield perpendicularly aligned cells. Indium-tin-oxide layers deposited on glass by standard r.f. sputtering also produce perpendicular alignment after exposure to fluorine free radicals, however a complication arises. Fluorine incorporated in the ITO film decreases the free electron concentration either by acting as a trap or by filling oxygen vacancies. The resistivity of the conducting film increases sharply. This has been accounted for by considering the diffusion of active species into the thin film.<sup>1</sup> While such cells can still be used for measurements, the high resistivity of the conductive layer is quite detrimental. It is better to replace the tetrafluoromethane plasma with tetrafluoroethylene which is known to produce a teflon-like polymer.<sup>7</sup> Conditions are arranged to minimize polymerization in the gas phase and favor in situ polymerization at the substrate surface. Clear films are produced, nearly pinhole free and conforming to steps on the surface. ESCA spectra of these films show a main —CF<sub>2</sub>— peak and a minor —CH<sub>3</sub> peak and resemble the commercial polymer "teflon". The resistivity is at least 10<sup>12</sup> ohm cm and thus the film forms a true blocking layer. However, the film resistance is bypassed by its capacitance which is about 3 orders of 10 larger than the cell capacitance. The phase shift introduced by the film is negligible beyond 100 Hz. In contrast, an F· etched ITO cell acts as a series R/C circuit.

Figures 1a and 1b show the permittivity of cells made from substrates coated with polyfluorocarbon and filled with *n*-octylcyanobiphenyl (BDH K24). All cells are about 10 μM thick. In Figure 1a, the electrode pattern is etched in an ITO film, in Figure 1b, both sides are Cr/Au. The patterns are etched prior to the deposition of (CF<sub>2</sub>)<sub>n</sub>. Gold was chosen because it does not introduce strong alignment forces and therefore forms a convenient

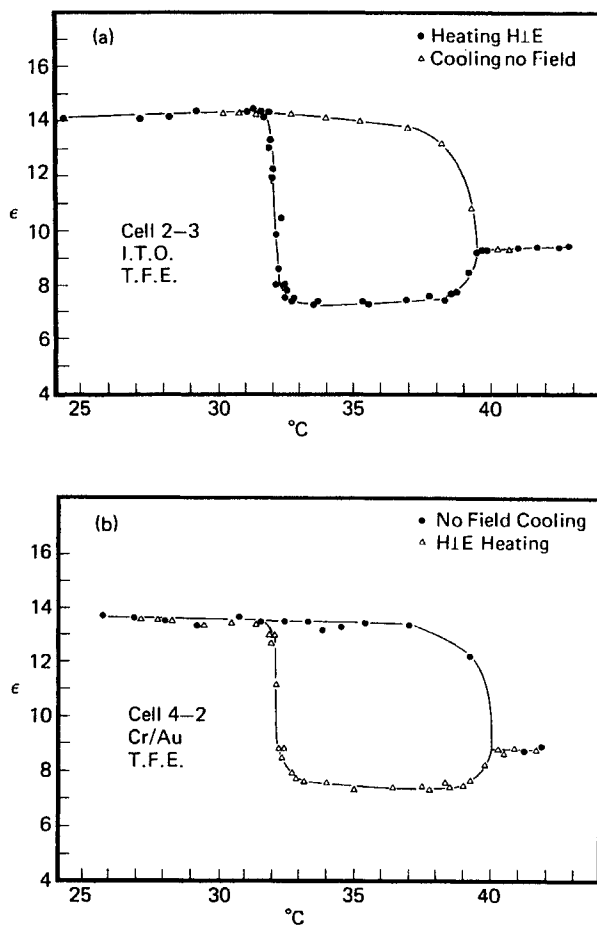


FIGURE 1 Permittivity of *n*-octylcyanobiphenyl as function of temperature for samples placed in a 12 kGauss H field. (1a) ITO electrodes, polyfluorocarbon coating. (1b) Cr/Au electrodes polyfluorocarbon coating.

reference surface. Figure 2 shows the permittivity of the same compound between Cr/Au electrodes cleaned only in warm chromic acid. All cells are filled at 50  $^{\circ}\text{C}$  using a vacuum filling technique. Upon cooling to room temperature, coated cells assume complete perpendicular alignment as evidenced by the extinction under the polarizing microscope. If the cell is heated in a magnetic field (13 kGauss) directed parallel to the electrode surface realignment occurs at the smectic A to nematic transition temperature (32  $^{\circ}\text{C}$ ). The permittivity drops from 14.1 to 7.4. The data points in Figure 1

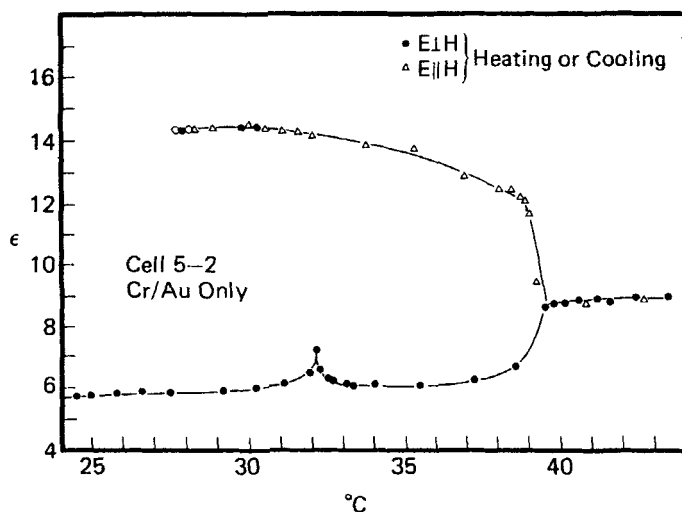


FIGURE 2 Permittivity of *n*-octylcyanobiphenyl as function of temperature as in Figure 1. Electrodes are cleaned Cr/Au.

clearly show that during the realignment the cell remains in equilibrium. Continuing through the nematic phase, the alignment remains under control of the H field until the temperature approaches the  $N \rightarrow I$  transition temperature ( $40^\circ\text{C}$ ). If the cell is cooled from isotropic while the magnetic field is directed perpendicular to the electrode surface the cell is aligned perpendicular throughout the nematic and smectic ranges. There is no change in  $\epsilon$  at the  $N \rightarrow \text{SmA}$  transition presumably only longitudinal alignment occurs as the sample changes to smectic. The  $\epsilon$  data for perpendicular aligned H fields are identical with those without the magnetic field. The polyfluorocarbon layer exerts aligning forces comparable in magnitude to the bulk forces of a strong magnetic field.

The Cr/Au cell in Figure 2 lacks strong build-in surface alignment and only the magnetic field determines the room temperature alignment. If the sample is cooled in an H field parallel to the surface, the smectic phase will end up parallel aligned. If the H field is perpendicular to the surface, the sample will be perpendicular at room temperature.  $\epsilon_1$  is about 14.1 for the coated cells and for the Cr/Au cell aligned by a perpendicular field but  $\epsilon_2$  is about 7.5 for the coated cells while for the Cr/Au cell  $\epsilon_2$  is about 6 in the nematic region, both cells aligned by a parallel field. This difference is much larger than the experimental error. Thus, a cell with perpendicular aligning surfaces placed in a strong H field parallel with the surface still has a considerable fraction of the liquid crystal in perpendicular alignment.

## 2 Parallel alignment

The simplest way to obtain alignment on glass or ITO surfaces is by exposing the etched substrate to  $O_2$  from an upstream  $O_2$  plasma. On r.f. sputtered ITO, perfect parallel alignment can be obtained but the technique has failed at times for commercial "NESA" glass of unknown origin. Figure 3a shows  $\epsilon(T)$  data for  $O_2$  etched r.f. sputtered ITO. Figure 5a shows the texture of the smectic phase. In the smectic phase the sample is parallel aligned,  $\epsilon_2$  is about 5.2 which is well below that of a Cr/Au cell. Heating in a magnetic field aligned perpendicular to the electrode surface produces perpendicular alignment in the nematic phase but  $\epsilon_1$  is about 10.8, as compared with  $\epsilon_1$  which is about 14.1 for complete perpendicular alignment. Again the nematic phase is only partially aligned; the surface forces oppose the bulk forces of the H field.

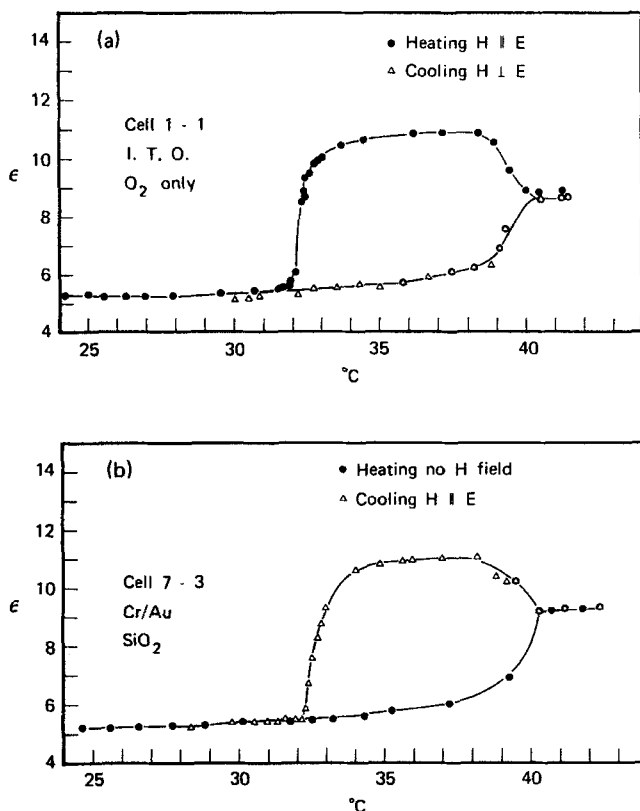


FIGURE 3 Permittivity of *n*-octylcyanobiphenyl as function of temperature for samples placed in a 12 kGauss H field. (3a) ITO electrodes, oxygen plasma etched. (3b) Cr/Au electrodes,  $SiO_2$  coating deposited by r.f. plasma.



Oxygen etching is applicable only to glass or ITO surfaces. For metal surfaces, deposition of  $\text{SiO}_2$  or  $\text{SnO}_2$  achieves the same parallel alignment found for  $\text{O}_2$  etched glass surfaces. The method is more general and produces acceptable results even on "poor" nesatron coatings. Figure 3b shows  $\epsilon(T)$  for a cell having Cr/Au electrodes covered with a thin film of  $\text{SiO}_2$ . The film is deposited by introducing a suitable silane compound into an  $\text{O}_2$  plasma. The compound is completely oxidized to  $\text{SiO}_2$ , thus, its chemical structure has no effect on the L.C. alignment. The choice is based on its vapor pressure; the cell in Figure 3b was made using bis(dimethylamino) dimethyl silane which has the desired vapor pressure at room temperature. The deposited film is clear and smooth. Incomplete oxidation and too rapid evaporation leads to yellow-brownish deposits having poor aligning properties. Figure 3b is almost identical with Figure 3a  $\epsilon_2$  is about 5.8 and  $\epsilon_1$  is about 10.9 at  $36^\circ\text{C}$  again showing incomplete alignment in a perpendicular field. Figure 5b shows the texture of a cell having Cr/Au,  $\text{SiO}_2$  on one electrode and ITO,  $\text{SiO}_2$  on the other. The photograph shows the edge of the circular Cr/Au electrode. Note that there is no change in alignment across this edge. The step introduced by the electrode layer is about  $1500 \text{ \AA}$ . The smectic compound seems to be able to bend that much without introducing dislocations.

### 3 Mixed alignment

Data presented so far indicate that either type of alignment, parallel or perpendicular, can be introduced at will. It is of interest to compare the two kinds of surface forces in a single cell. Cells having "mixed" alignment and filled with nematics have been discussed.<sup>8</sup> However, alignment was obtained by using a doping agent which cause homeotropic orientation. As before, the mixed aligned cells discussed here are not doped.

Figure 4 shows  $\epsilon(T)$  data for cells having Cr/Au electrodes, one of which is coated with  $\text{SiO}_2$ , the other with polyfluorocarbon. The liquid crystal material is again *n*-octylcyanobiphenyl. Data for  $\epsilon_1$  and  $\epsilon_2$  are now intermediate between those for all parallel cells and all perpendicular cells:  $\epsilon_1$  is about 13.0 and  $\epsilon_2$  is about 6.6 at  $36^\circ\text{C}$ . For mixed aligned cells the average orientation in the smectic phase is not determined solely by the surface forces as was the case in the previous examples. Some of the orientation produced by the magnetic field persists through the  $\text{N} \rightarrow \text{SmA}$  transition but to a much smaller extent than was observed in Figure 2 for cells without surface interaction. If mixed aligned cells are cooled from isotropic without a magnetic field  $\epsilon$  is about 9.6 at room temperature, cooled in a magnetic field perpendicular to the surface  $\epsilon$  is about 10.8 and for a parallel field  $\epsilon$  is about 8.5.

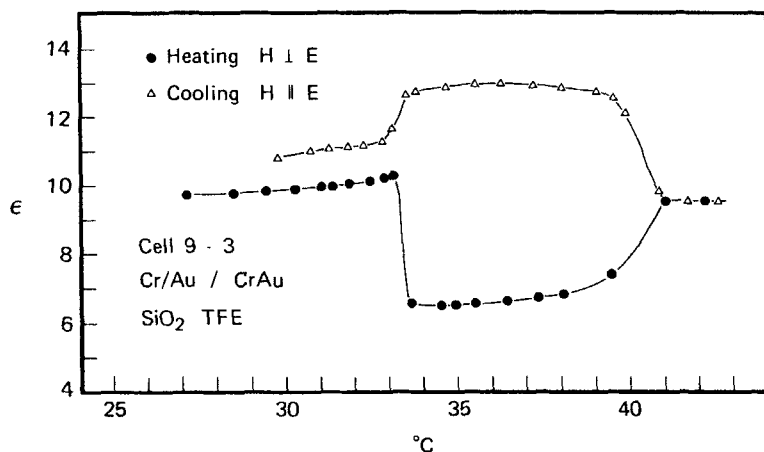


FIGURE 4 Permittivity of *n*-octylcyanobiphenyl as function of temperature for samples placed in a 12 kGauss  $H$  field. Cr/Au electrodes one side coated with  $\text{SiO}_2$ , the other side with T.F.E. This produces "mixed" alignment.

Figure 5c shows the texture of such cells in the smectic phase. This texture scatters light strongly. When the cells cool through the phase transition the smectic phase cannot sustain the bend introduced by the surface and the phase breaks up into small domains of different orientation causing the strong scattering.

#### 4 Threshold data

Figure 6 shows the measured  $\epsilon(H)$  curves for the three types of cells: parallel, perpendicular and mixed alignment. All data were taken at  $36^\circ\text{C}$ , the middle of the smectic range. The thresholds for parallel and perpendicular cells are rather large, nearly 4 kGauss. The mixed aligned cell does not have a threshold in the mathematical sense,  $\epsilon$  is a continuous function of  $H$  for any value of  $H$ . Nevertheless the  $\epsilon(H)$  function for those boundary conditions is a rather weak function for small values of  $H$  as will be shown in the next section. For mixed aligned cells one can obtain  $\epsilon(H)$  data for both directions of  $H$ . As is indicated in Figure 6, below about 1 kGauss the data for parallel and perpendicular oriented  $H$  fields are the same within experimental error.

#### DISCUSSION

The experimental results can be summarized as follows: A thin film of poly-fluorocarbon deposited on both walls of the cell cause perpendicular alignment of the liquid crystal body equal to (and perhaps exceeding) the align-

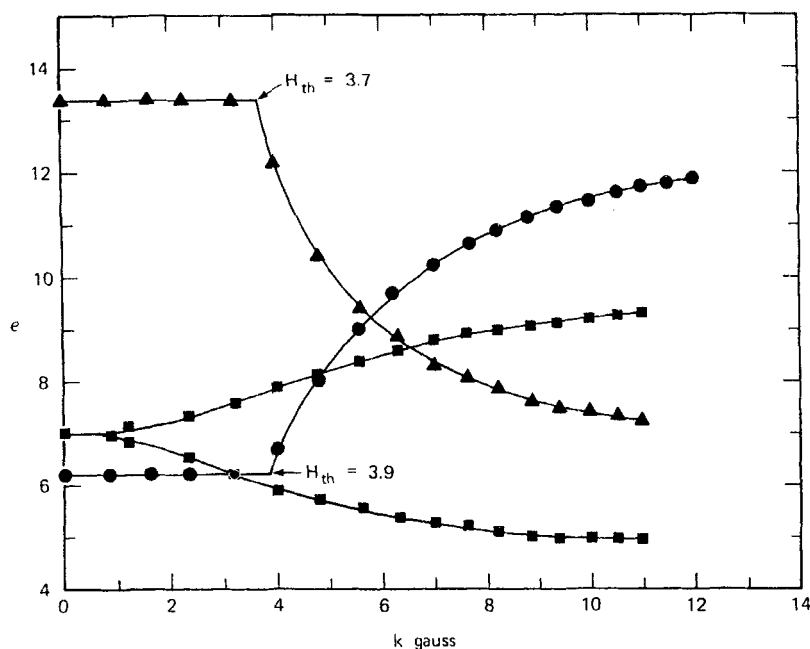


FIGURE 6 Permittivity vs. H field for: (a) parallel wall alignment H perpendicular to the surface; (b) perpendicular wall alignment H parallel with the surface; (c) and mixed alignment H perpendicular and H parallel with the surface.

ment which can be obtained by placing an untreated cell in a strong magnetic field directed perpendicular to the surface. For coated cells  $\epsilon_1$  of octylcyanobiphenyl is about 14; for cells with clean Cr/Au electrodes in a 13 kGauss field  $\epsilon_1$  is about 13.5.

Similarly, thin films of  $\text{SiO}_2$  or  $\text{SnO}_2$  deposited on both walls of the cell cause parallel alignment of the liquid crystal-body at least equal to that which is obtained by putting an untreated cell in a strong magnetic field directed parallel with the surface. For coated surfaces  $\epsilon_2$  is about 5.8 while for neutral surfaces, placed in a parallel magnetic field  $\epsilon_2$  is about 6.0.

If the magnetic field is orthogonal to the surface induced orientation, the effect of the surface is still quite evident: for perpendicular surface orientation but parallel H field  $\epsilon_2$  is 7.5 as compared to 5.8 for the untreated surface. For parallel surface orientation and perpendicular H field  $\epsilon_1$  is 10.8 as compared to 13.5 for a clean Cr/Au surface.

For "mixed" aligned cells, having a parallel orienting surface on one side and a perpendicular orienting surface film on the other side both  $\epsilon_1$  and  $\epsilon_2$  are intermediate but the cell does not behave as an untreated cell.

If the surface changes the alignment of the liquid crystal body there must be a change in the Gibbs' free energy of the liquid crystal. Following A. Saupe<sup>9</sup> most authors have introduced the surface-liquid crystal interaction as a boundary condition reflecting the orientation of the L.C. at the surface. A. Rapini *et al.*<sup>10</sup> and others have considered more complicated boundary conditions but still the effect of the surface interaction is not represented in the usual expression for the free energy of the system. While the existing theory agrees well with experiment for all-parallel or all-perpendicular wall alignment, it is not consistent with data for mixed aligned cells. This is exemplified briefly in the remainder of this section, a more comprehensive account is left to a future paper.

The permittivity of a distorted nematic, in terms of the principal components  $\epsilon_1$  and  $\epsilon_2$  is given by

$$\epsilon^{-1} = \int_0^1 (\epsilon_1 \cos^2 \phi + \epsilon_2 \sin^2 \phi)^{-1} dx \quad (1)$$

where the  $x$ -axis is taken perpendicular to the electrode surface and  $x$  is normalized with respect to the cell thickness  $d$ .  $\phi(x)$  is the angle between the director  $L$  and the positive  $x$ -axis.  $\epsilon_1$  is parallel with  $L$ ,  $\epsilon_2$  is the perpendicular component. Expression (1) follows from Maxwell equations as was shown by H. Gruler *et al.*<sup>11</sup> and H. Deuling.<sup>21</sup> H. Onnagawa *et al.*<sup>13</sup> give a less exact derivation.

The function  $\phi$  is a solution of the second order equation:

$$\phi''(x) \pm A \sin \phi \cos \phi = 0 \quad (2)$$

where the  $+$  sign refers to the case  $H$  parallel with the electrode surface and the  $-$  sign refers to  $H$  perpendicular to the surface. The parameter  $A$  is given by

$$A = \frac{d^2 H^2 \Delta\chi}{k} \quad k = k_{11} = k_{33}. \quad (3)$$

Equation (2) follows in the usual way by minimizing the integral expression for the free energy using the Euler-La Grange technique and putting  $k_{11} = k_{33}$ .<sup>11</sup> Equation (2) is solved numerically and the resulting vector  $\phi, x$  is used to evaluate the integral equation (1). An analytical solution is known for boundary conditions appropriate to parallel or perpendicular wall alignment but not for the mixed aligned cell. The numerical technique can be used with any sufficient set of boundary values.

## 1 Perpendicular alignment

The analytical solution for the boundary conditions:

$$\begin{aligned}\phi'(x = \tfrac{1}{2}) &= 0 \\ \phi(x = 0) &= 0\end{aligned}\quad (4)$$

is an elliptic integral of the first kind. The boundary conditions reflect the assumptions:

- The deformation is symmetrical and  $\phi$  and its derivatives are continuous.
- The wall alignment is not changed if an  $H$  field is applied.

The elliptic integral must be evaluated numerically and therefore it seems more direct to solve equation (2). The computer program is based on the Runge Katta technique.<sup>14</sup> Figure 7 exemplifies the results for perpendicular wall alignment and the boundary conditions mentioned above. In Figure 7  $\phi(x)$  is plotted for selected values of the parameter  $A$ . Within the context of the R.K. program each curve is uniquely determined by a single parameter  $\phi_m = \phi(x = \frac{1}{2})$  since for all curves  $\phi'(x = \frac{1}{2}) = 0$ . It is instructive to plot  $\phi_m$  vs.  $A$  as in Figure 8. For  $\sqrt{A} = \pi + \delta$   $\phi_m$  is a strong function of  $A$  and for  $\sqrt{A} \leq \pi$   $\phi_m = 0$ . This is of course well known from the properties of elliptic integrals of the first kind. Thus for these boundary conditions the numerical

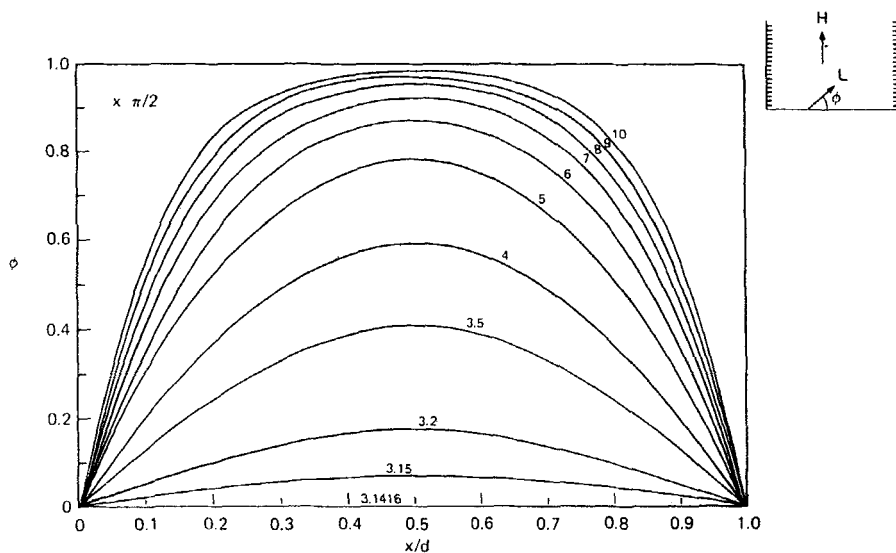


FIGURE 7  $\phi$  vs.  $x/d$  for  $\sqrt{A} = 3.1416, 3.15, 3.2, 4, \dots, 10$ . For  $\sqrt{A} \leq \pi$  the computer program finds  $\phi_m < 10^{-17}$ . Perpendicular wall alignment,  $H$  parallel with the electrode surface. For parallel wall alignment and  $H$  perpendicular to the surface the  $\phi(x)$  data are complementary.

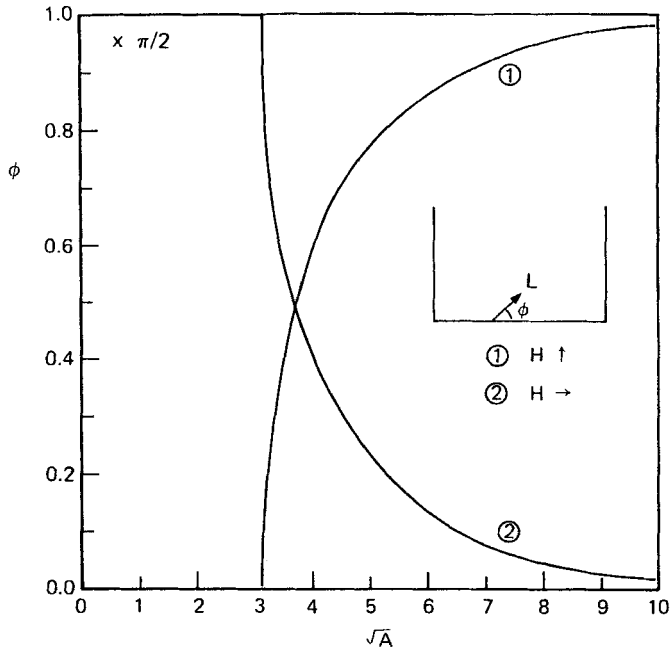


FIGURE 8  $\phi_m$  vs.  $\sqrt{A}$ . Curve 1: perpendicular wall alignment  $H$  parallel with electrode surface. Curve 2: parallel wall alignment and  $H$  perpendicular to the surface.

procedure yields the same results as the analytical solution and as before there is a threshold for:

$$\pi = \sqrt{A} = H_{th} \cdot d \cdot \sqrt{\frac{\Delta\chi}{k}} \quad (5)$$

Having determined  $\phi(x)$  for a set of values for  $A$  one can integrate equation (1) and plot  $\varepsilon$  vs.  $\sqrt{A}$  as in Figure 9. Comparison with experimental data in Figure 6 can be made by scaling the abscissa in Figure 6 according to

$$\sqrt{A} = \pi \frac{H}{H_{th}} \quad (6)$$

It is seen that good agreement is obtained.

## 2 Parallel alignment

Substitution  $\psi = \phi + \pi/2$  converts equation (2) and the boundary conditions from those for perpendicular to those for parallel alignment. Therefore all  $\phi(x)$  for the parallel case are complementary to those for the perpendicular

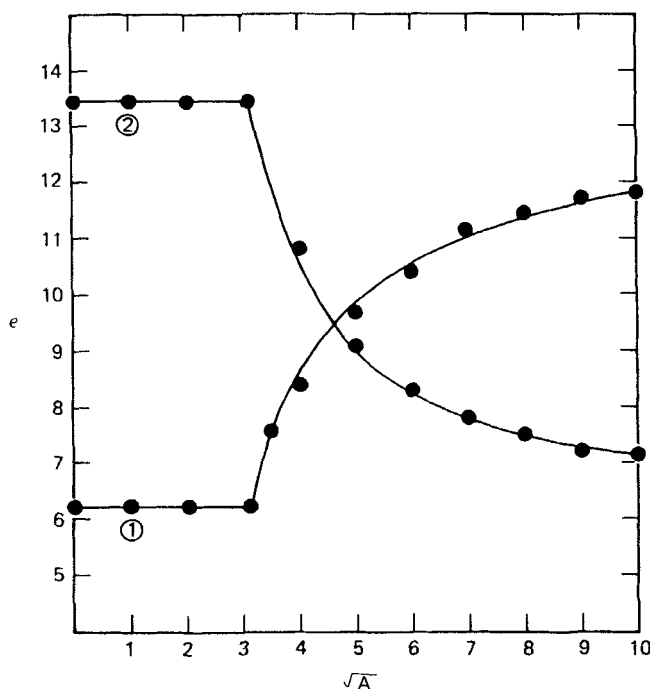


FIGURE 9 Calculate values for  $\varepsilon$  vs.  $\sqrt{A}$  at  $36^\circ\text{C}$ .  $\varepsilon_1 = 13.4$  (polyfluorocarbon cells) and  $\varepsilon_2 = 6.2$  ( $\text{SiO}_2$  cells). Curve 1: parallel surface alignment and  $H$  perpendicular to the surface. Curve 2: perpendicular wall alignment and  $H$  parallel with the surface. Experimental data from Figure 6 are replotted by changing the abscissa according to  $\sqrt{A} = \pi \cdot H/H_{\text{th}}$ .

case. The required changes in the program were made and this was verified. As before one calculates the  $\varepsilon(\sqrt{A})$  curve and comparison with experiment is made by scaling the abscissa in Figure 6. The results are plotted in Figure 9 and good general agreement is noted.

### 3 Mixed alignment

Agreement between experimental results for perpendicular or parallel wall alignment and the analytical solution of equation (2) has been observed before.<sup>11</sup> Therefore the above establishes the fact that the numerical technique is essentially correct. For mixed alignment, where the analytical approach fails, the numeric technique yields the results plotted in Figure 10. As before,  $\phi(x)$  is plotted for values of  $\sqrt{A} = 0, 1, \dots, 10$ . The figure refers to parallel wall alignment at  $x = 0$ , perpendicular alignment at  $x = 1$  and  $H$  directed parallel with the cell walls. For  $H$  perpendicular to the cell walls one obtains

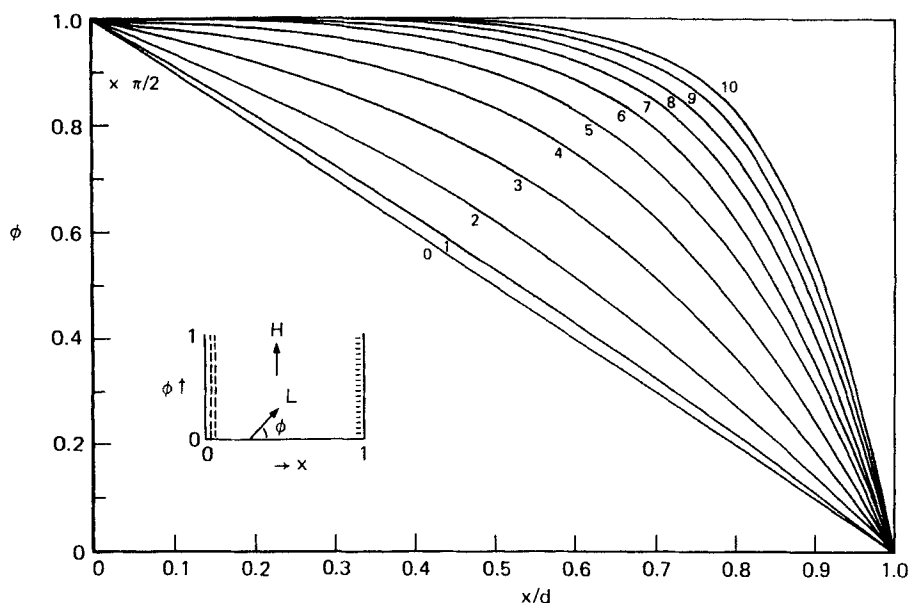


FIGURE 10  $\phi(x)$  for  $\sqrt{A} = 0.1, \dots, 10$  for mixed aligned cells and  $H$  parallel with the cell walls.

$\phi(x)$  data which are complementary as will be evident by substituting  $\psi \rightarrow \phi + \pi/2$ . All curves are now uniquely characterized by the starting slope  $\phi'(0)$  or  $\phi'(1)$  and these slopes turn out to be continuous functions of  $A$ . However, for small  $A$  this is only a weak function. Calculated values for  $\varepsilon$  for both directions of the  $H$  field are plotted in Figure 11. For  $\sqrt{A} < 1$  experimental uncertainty does not permit to distinguish between the two  $\varepsilon$ 's. Comparing the theoretical curves in Figure 11 with the experimental data in Figure 6 it is seen that the general slope of the curves agrees. However, the experimental data are well below the calculated values. The average  $\varepsilon$  of the cell (without external field) is 7 while the calculated value is 9. The theory indicates that for a mixed aligned cell  $\phi(x)$  changes linearly with  $x$  from 0 to  $\pi/2$  which leads to  $\varepsilon = 9$ . The experimental data indicate that  $\phi(x)$  is given by a curve characterized by  $\sqrt{A} = 4$  or 5 (for  $H$  parallel with the surface). Thus for a mixed aligned cell the parallel wall alignment extends for a considerable distance into the cell and  $\phi(x)$  is not linear in  $x$ .

This can be accounted for by introducing a surface term reflecting the dipole interaction at the surface. It can be shown that this does not alter the results for all-parallel or all-perpendicular wall alignment it only changes the numerical value of  $k$ . Alternatively, within the existing theory one could



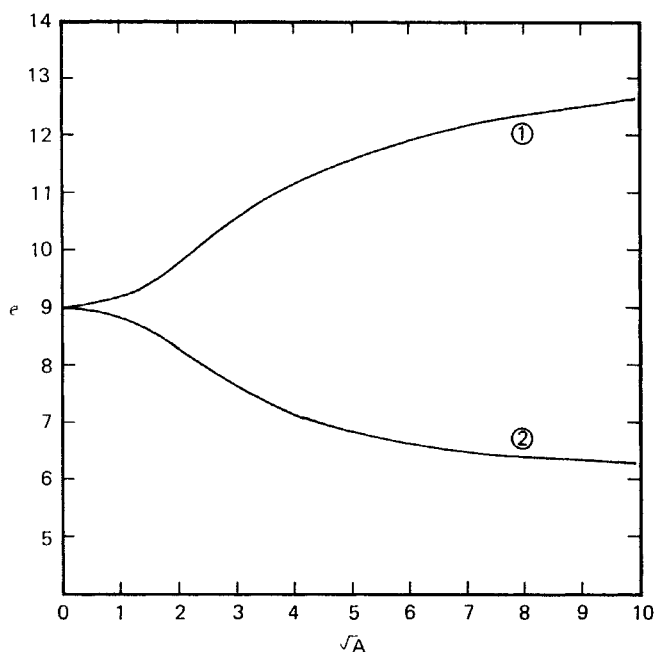


FIGURE 11  $\epsilon$  vs.  $\sqrt{A}$  calculated for mixed aligned cells. Curve 1: H field perpendicular to the electrode surface. Curve 2: H field parallel with the surface.

obtain lower values for  $\epsilon$  by letting  $\phi(1) > 0$  however, this would (a) contradict the results for all-perpendicular alignment and (b) it would mean that boundary conditions on one surface are related to those at the other surfaces.

## SUMMARY

Thin films deposited by r.f. plasma techniques and r.f. plasma etched glass surfaces have unique aligning properties. Oxide surfaces, examples  $\text{SiO}_2$  and  $\text{SnO}_2$ , produce parallel alignment for alkylcyanobiphenyls. Poly-fluorocarbon films force perpendicular alignment. The surface-liquid crystal interaction is quite strong as evidenced by the high threshold values for Fréedericksz transitions, about 4 kGauss. The strong wall forces make it possible to produce mixed aligned cells without adding dopants.

Experimental  $\epsilon(H)$  curves were analyzed using existing theory, solving the differential equations numerically. Good agreement is obtained for all-parallel or all-perpendicular alignment but the theory fails to account for

the  $\varepsilon(H)$  data for mixed aligned cells. While theory predicts a linear change in the aligning angle with distance, the experiment indicates that parallel alignment extends over a considerable distance into the cell. Appropriate changes in the theory are indicated but a full account is postponed to Part II of this paper.

### Acknowledgments

Among those who have contributed to this program I want to mention in particular: Dr. Vance Hoffman, Dr. J. R. Hollahan and R. M. Gibson.

### References

1. G. J. Sprokel and R. M. Gibson, *J.E.C.S* 124(4) 557 (1977).
2. *Techniques and Applications of Plasma Chemistry*, Ed. J. R. Hollahan, Alexis T. Bell, Wiley, 1974.
3. Ivan Haller, *Progress in Solid State Chemistry*, 10, 103 (1975).
4. Tegal Co., Richmond, California 94804.
5. J. C. Dubois, M. Gazard, and A. Zanu, *APL*, 24, 297 (1974).
6. G. J. Sprokel, *Mol. Cryst. Liq. Cryst.*, 22, 249 (1973).
7. M. Milard in Chapter 5 of Reference 2.
8. K. Fahrenschon, H. Gruler, and M. F. Schieckel, *Appl. Phys.* (Springer), 11, 67 (1976).
9. A. Saupe, *Z. Naturforsch*, 15a, 815, 1960.
10. A. Rapini and M. Papoular, *J. Phys.*, (Paris) C4-54, (1969).
11. H. Gruler, T. J. Scheffer, and G. Meier, *Z. Naturforsch*, 27a, 966 (1972).
12. H. Deuling, *Mol. Cryst. Liq. Cryst.*, 19, 123 (1972).
13. H. Onnagawa and K. Miyashita, *J.A.P. (Japan)*, 13, 1741 (1974); *J.A.P. (Japan)*, 14, 1061 (1975).
14. J. B. Scarborough, *Num. Math. Analysis*, John's Hopkins (1966).